Hindawi
International Journal of Photoenergy
Volume 2021, Article ID 6935269, 10 pages
https://doi.org/10.1155/2021/6935269

Research Article

Aloe-Emodin-Mediated Photodynamic Therapy Induces Apoptosis in Basal Cell Carcinoma Cells via Activation of ERK/JNK Signaling Pathway

Woodvine Otieno Odhiambo,[1] Songmei Geng,[2] Xiaopeng Wang,[2] Xiaodong Chen,[1] Mengting Qin,[1] Meng Yuan,[1] Yang Wang,[1] Farooq Riaz,[3] Chengcheng Liu,[1] and Yanhong Ji[1]

[1]*Department of Pathogenic Microbiology & Immunology, School of Basic Medical Sciences, Xi'an Jiaotong University Health Science Center, 76 West Yanta Road, Xi'an 710061, China*
[2]*Department of Dermatology, The Second Affiliated Hospital of College of Medicine, Xi'an Jiaotong University, 157 Xi Wu Road, Xi'an 710004, China*
[3]*Department of Biochemistry & Molecular Biology, School of Basic Medical Sciences, Xi'an Jiaotong University Health Science Center, 76 West Yanta Road, Xi'an 710061, China*

Correspondence should be addressed to Chengcheng Liu; liuchengcheng@xjtu.edu.cn and Yanhong Ji; jiyanhong@xjtu.edu.cn

Received 20 April 2021; Accepted 21 September 2021; Published 9 November 2021

Academic Editor: Alberto Álvarez-Gallegos

Basal cell carcinoma (BCC) is the most prevalent epidermal cancerous neoplasm. Previous studies have reported the noninvasive, cost-effective, and localized photodynamic therapy (PDT) approach to BCC treatment. This study investigated the photodynamic effects of aloe-emodin (AE), a natural anthraquinone photosensitizer (PS), on proliferation and apoptosis of BCC TE 354.T cell line. To evaluate the effects of AE-mediated PDT, we used various concentrations of AE (0, 2.5, 5, and 10 μM) and white light energy (0, 12, 24, and 36 J/cm^2). CCK-8 assay was used to analyse cell viability following AE-mediated PDT. The cell death rate and reactive oxygen species (ROS) were assessed by flow cytometry. Western blotting was used to determine the effects of AE-mediated PDT on the apoptotic proteins, Akt, and MAPK pathways. AE-mediated PDT inhibited tumorigenic cell proliferation, consequently enhancing apoptosis in AE and PDT concentration and dose-dependent manner, respectively. Significantly increased TE 354.T cell apoptosis and intracellular ROS production were both observed after AE-mediated PDT. Following the AE-mediated PDT, cytochrome and antitumor p53 were elevated; however expression of Bcl-2 was significantly decreased. Significant caspase 3 elevation post-AE-mediated PDT suggested intrinsically driven apoptosis. Additionally, AE-mediated PDT significantly suppressed NF-κB, Akt, and ERK pathways while JNK expression was significantly increased. AE-mediated PDT induced TE 354.T cell apoptosis through the intracellular generation of ROS. Akt, ERK, and JNK all play various roles in ensuring successful TE 354.T tumor cell apoptosis.

1. Introduction

Basal cell carcinoma (BCC) is a slow-growing and locally invasive skin tumor, specifically on the epidermal surface [1, 2]. BCC remains the most prevalent global cancerous neoplasm with an increased incidence in the last decade [3]. Various factors such as closeness to the equator and an aging global population increase the risks and make any race vulnerable, with doubling incidences from 40 to 70 years [4, 5]. BCC may damage the neighbouring tissues and have a relatively high reoccurrence rate in 10-20% of the successfully treated and recovered patients [6]. Various methods of treatment have been used, with surgery being considered the gold standard [7]. However, BCC often occurs on the

neck, face, or extremities, and cosmetic preference warrants an alternative noninvasive therapeutic mode [6].

Photodynamic therapy (PDT) is a promising site-specific, less-invasive, and cost-effective interventional approach for malignant tumor treatment [1, 7–9]. PDT depends on the stimulation of a photosensitizer (PS) by a light source with an appropriate wavelength that generates superoxide anion ($O_2^{-}\bullet$), hydroxyl radicals (OH•), and hydrogen peroxide (H_2O_2) through a type I reaction or singlet oxygen ($^1O_2$) through a type II reaction. These reactive oxygen species (ROS) can induce tumor cell death [10]. Several PSs have been reported to effectively kill BCC cells under light irradiation, and 5-aminolevulinic acid (5-ALA) and methyl aminolevulinate (MAL) have been tried for photodynamic treatment of BCC in clinical practice.

Aloe-emodin (1,8-dihydroxy-3-hydroxymethyl-anthraquinone, AE, Figure 1) is a natural anthraquinone compound isolated from *Aloe barbadensis Miller* and *Rheum palmatum L* [11]. The antitumor activity of AE and its apoptosis inducing effects in various deep-seated tumors such as colon cancers has been reported. Additionally, AE and PDT combination has been shown to significantly suppress metastasis of HUVEC [12], human oral mucosa carcinoma [13], and MG63 osteosarcoma cell line [14]. We have also reported that AE-mediated antimicrobial photodynamic therapy could effectively inactivate drug-sensitive and drug-resistant *Candida albicans* [15]. AE exhibits fluorescence and has a maximum excitation wavelength (430 nm), hence a novel PS [12]. In addition, its maximum absorption peak in the blue region could enhance its photosensitizing ability for the treatment of superficial diseases [16]. The photocytoxicity of aloe-emodin has been reported to occur in human skin fibroblast through the cellular DNA and RNA oxidative damage [17]. However, the AE-mediated PDT effects on BCC remain unclear. Consequently, this study evaluated the AE-mediated photodynamic effects on proliferation and apoptosis of BCC TE 354.T cell line. As a tumor under the skin, the authors believe this would be a feasible BCC therapeutic regimen.

2. Materials and Methods

2.1. Photosensitizer. AE was purchased from Nanjing Jinzhu Biotechnology Co. Ltd, China. AE was dissolved in dimethyl sulfoxide (DMSO) (Sigma-Aldrich, USA) to prepare a 1 mM stock solution. The AE stock solution was further diluted to desired concentrations (2.5, 5, and 10 μM) with Dulbecco's modified Eagles medium (DMEM, Hyclone, USA), which was immediately used for subsequent experiments. All the photodynamic assays were carried out through the use of white light. The wavelength of 435 ± 10 nm for the irradiation was selected by a 50 W xenon lamp (Ceaulight CEL-HXF-300, China), and this lamp was equipped with an optical filter. The distance between the samples and light source was 10 cm. Light fluency rate at the level of samples was adjusted to 40 m/W cm^{-2} by a power meter (Ceaulight NP-2000, China). To control sample heating, ice-cold water filter with a width of 1 cm was inserted between the light source and the samples.

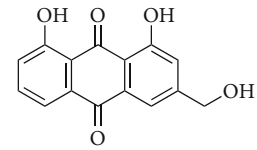

Figure 1: The chemical structure of aloe-emodin.

2.2. Cell Line and Culture Conditions. BCC TE 354.T cell line (ATCC CRL-7762) was purchased from BeNA Culture Collection (BNCC337678, Beijing, China). The cells were cultured in DMEM supplemented with 10% fetal bovine serum (Zhengjiang Tianhang Biotechnology, China), 100 U/ml of penicillin, and 100 μg/ml of streptomycin (Hyclone, USA) at 37°C in 5% CO_2 atmosphere. TE 354.T cells were plated in 96-well plates (Corning, USA) at a density of 5×10^3 cells per well and cultured overnight.

2.3. Photodynamic Treatments and Cell Proliferation Assay. TE 354.T cells were divided into four groups. The first group of cells was neither treated with AE nor irradiated (negative control, P-L-). The second group was treated with different concentrations (0, 2.5, 5, and 10 μM) of AE in the dark (P+L-). The third group of cells was irradiated with 435 ± 10 nm of white light for 5, 10, and 15 min, corresponding to the light energy doses of 12, 24, and 36 J/cm^2, respectively (P-L+). The fourth experimental cell group was treated with 0, 2.5, 5, and 10 μM of AE and irradiated with 12, 24, and 36 J/cm^2 of white light (P+L+). The cells incubated with DMEM containing less than 1% of DMSO (v/v) were also used as the negative control. After further 12 h incubation at 37°C in 5% CO_2 atmosphere, 10 μL CCK-8 (Beijing 4A Biotechnology, China) solution was added in each well. The plate was incubated at 37°C for 1 h, and the absorption values at 450 nm were determined by a microplate reader (BioRad, USA). Cell survival rate was calculated using the following equation, and each assay was repeated three times.

$$\text{Cell survival rate}(\%) = \left(1 - \frac{\text{Abs}_{(\text{no treatment})} - \text{Abs}_{(\text{PDT treatment})}}{\text{Abs}_{(\text{no treatment})} - \text{Abs}_{(\text{medium})}}\right) \times 100\%. \quad (1)$$

2.4. Cell Apoptosis. Apoptosis of TE 354.T cells was determined using Pharmingen™ PE Annexin V apoptosis detection kit (BD, USA) and Beckman Coulter CytoFLEX flow cytometer (Beckman, USA). In summary, approximately 1×10^6 cells in 2 mL DMEM were seeded in 6-well plates (Corning, USA). The cells were then treated with 5 μM AE and irradiated with light for 10 min (24 J/cm^2). The cells were subsequently incubated at 37°C for 12 h. PE Annexin V apoptosis detection kit was used for apoptosis assessment according to the guidelines of the manufacturer, and data was analysed using a flow cytometer.

2.5. Intracellular ROS. Approximately 1×10^6 TE 354.T cells seeded in 6-well plates were incubated with 5 μM of AE at 37°C 4 h and irradiated with light 10 min (24 J/cm^2). Cells were then resuspended in phosphate-buffered saline (PBS),

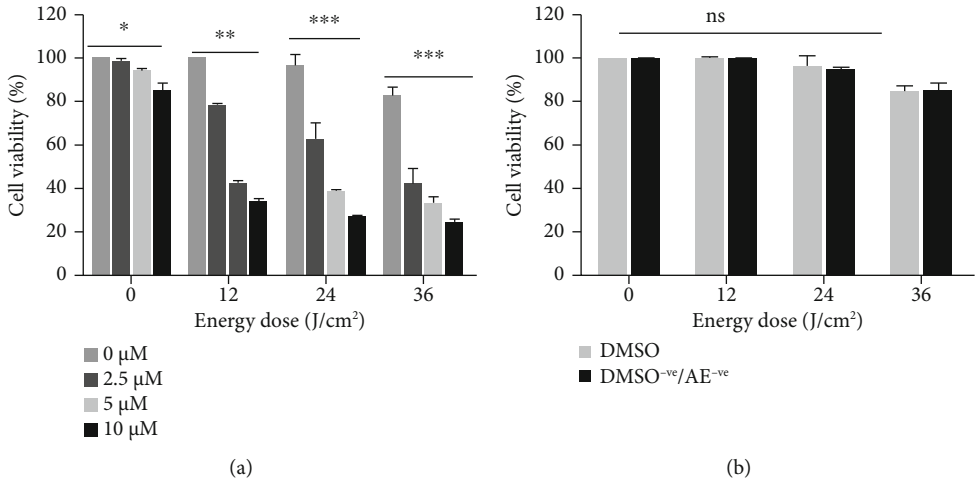

Figure 2: The viability of TE 354.T cells after AE-mediated PDT treatment. (a) Percentage of TE 354.T cell viability after treatment with varied AE concentrations and light energy doses. The photosensitizer at concentrations of 0, 2.5, 5, and 10 μM were introduced into the adhered cells for 4 hours and later irradiated with 0, 12, 24, and 36 J/cm^2. Cell viability was analysed 12 h postirradiation by CCK-8 kit ($^*p < 0.05$, $^{**}p < 0.01$, and $^{***}p < 0.001$); (b) viability of ATCC TE 354.T cell in the control group. The cells were incubated for 4 hours with either DMSO or without any treatment. The cells were exposed to irradiation with an energy dosage of 0, 12, 24, or 36 J/cm^2. No significant difference was reported between the two control groups at any given dosage of energy ($p > 0.05$).

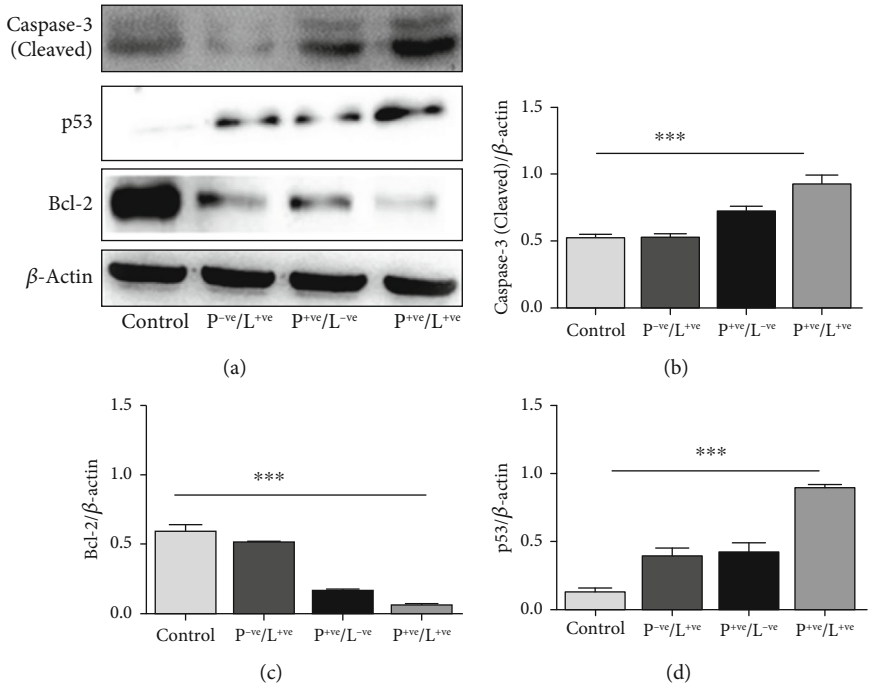

Figure 3: Western blotting expression of apoptotic proteins in TE 354.T cells following AE-mediated PDT. (a) The cells were treated with 5 μM AE, irradiated for 10 min, and protein lysates were collected 12 hours later for western blotting assays. (b–d) Quantitative analyses of change of cleaved caspase 3, Bcl-2, and p53, respectively ($^{***}p < 0.0001$). Protein level was expressed as mean ± SD from three independent experiments. Control (P-L-), light irradiation only (P-L+), AE only (P+/L-), and AE-mediated PDT (P+L+).

incubated with 5 μM of H2DCFDA (MCE, China) at 37°C in the dark for 30 min, and analysed in a flow cytometer. TE 354.T cells treated with 10 mM of hydrogen peroxide (H_2O_2) were used as the positive control.

2.6. Immunoblot Assays. Cell pellets after AE-mediated PDT treatment were harvested and lysed in radioimmunoprecipitation (RIPA) buffer, sonicated with a Bioruptor (Diagenode, Belgium). After centrifugation at 4°C, 13000 rpm for 20 min, the supernatant was collected. For electrophoresis, the protein sample lysates (40 μg) were loaded onto 10% (w/v) SDS-PAGE gel and transferred to polyvinylidene fluoride (PVDF) membrane (Millipore, USA). The membrane was subsequently blotted and probed with anti-caspase 3

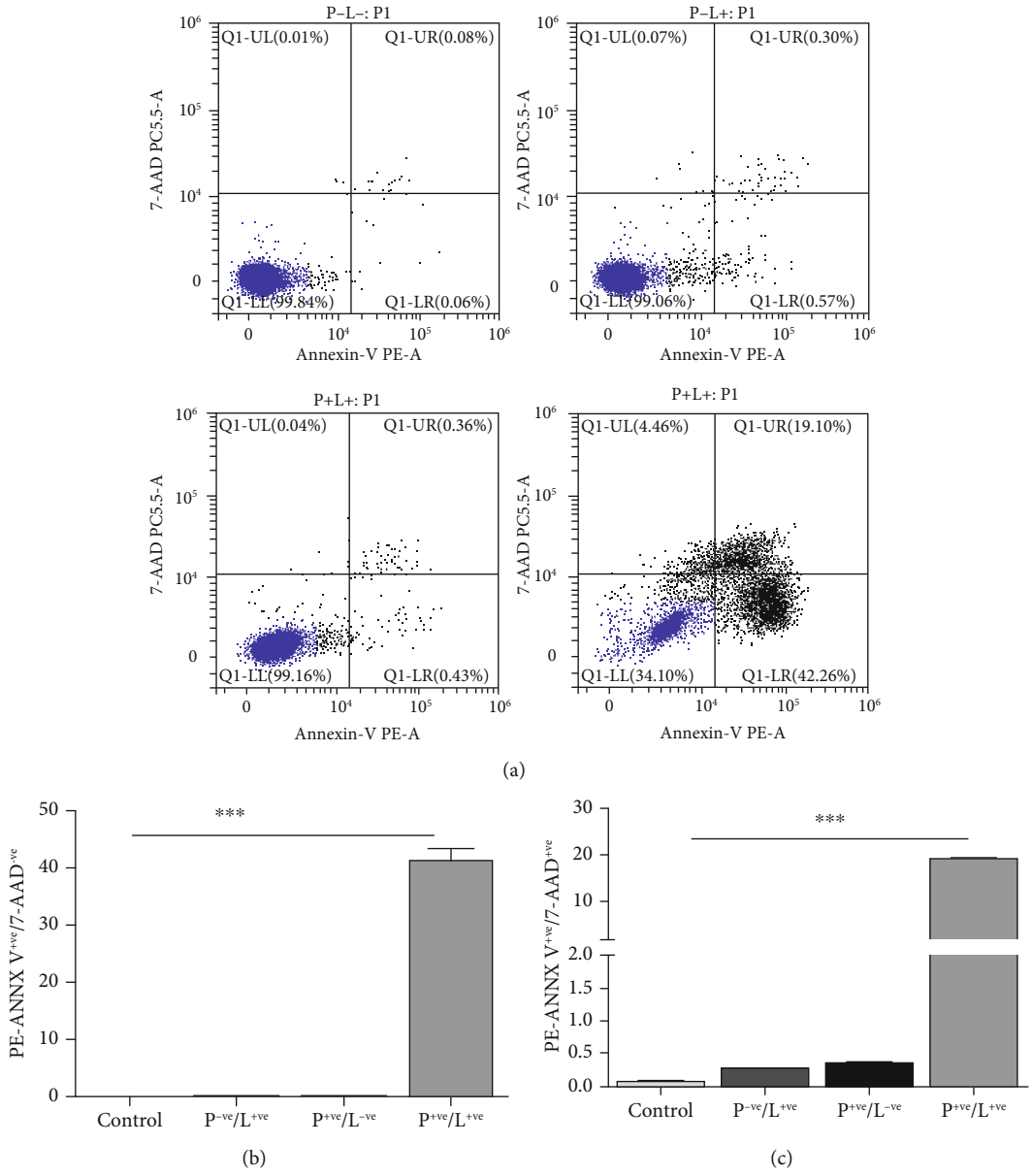

Figure 4: AE-mediated PDT consequences on cell apoptosis obtained through PE. (a) Annexin V/7-AAD staining and flow cytometry. Percentage graphical representation of PE-Annexin V positive cells' (b) early apoptosis and (c) overall apoptosis. The data show means ± SD of three independent assays (***$p < 0.0001$). Control (P-L-), light irradiation only (P-L+), AE only (P+/L-), and AE-mediated PDT (P+L+), respectively.

(Abcam 13586, UK), anti-c-Jun N-terminal kinases (JNKs), anti-p-JNK, anti-Bcl-2, anti-cytochrome C, anti-Akt, anti-p-Akt, anti-extracellular signal-regulated kinase (ERK), anti-p-ERK, and anti-p53 (CST, USA). The usage of a housekeeper gene, β-actin, was ensured as an internal control. Horseradish peroxidase (ThermoFisher, USA) conjugated goat anti-rabbit, and goat anti-mouse secondary antibodies were then used for signal detection. The bands were finally visualised using Immobilon™ Western Chemiluminescent HRP substrate (Millipore, USA). Three independent assays were performed, and data were analysed using ImageJ software and GraphPad Prism software.

2.7. Statistical Analysis. At least three independent experiments were done where stated. All data were analysed using the GraphPad Prism software and shown as the mean ± standard deviation (SD). Data were compared using one-way or two-way ANOVA, and the difference was considered significant in the case of $p < 0.05$.

3. Results

3.1. AE-Mediated PDT Cytotoxicity on TE 354.T Cells. The temperature of the samples prior to irradiation was 36.1°C. After irradiation, the temperature dropped to 35.2°C, implying

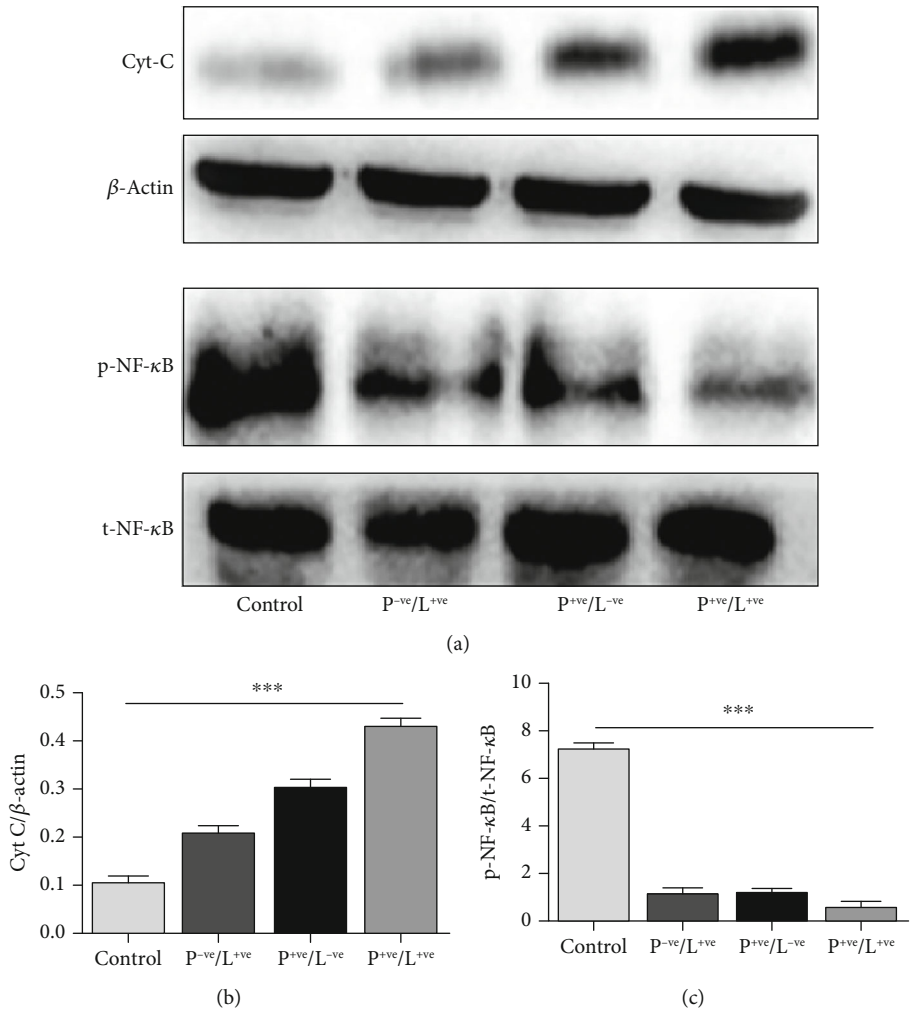

Figure 5: (a) Western blotting expression of cytochrome C and TNF-$\kappa\beta$ in TE 354.T cells following AE-PDT. The cells were treated with 5 μM AE, irradiated for 10 min, and protein lysates were collected 12 h later for western blotting assays. β-Actin was used as an internal control. The graphs represent the quantitative analysis of (b) cytochrome C changes relative to β-actin and (c) p-NF-κB relative to total TNF-kB. $^{***}p < 0.0001$. Protein level was expressed as mean ± SD from three independent experiments.

that the samples were not heated by light. Various treatments lead to change of cell viability as shown in Figure 2(a). AE alone (2.5 μM, 5 μM, and 10 μM) resulted to insignificant change of cell viability at 98.40 ± 0.79%, 93.37 ± 1.05%, and 84.40 ± 2.41%, respectively ($p > 0.05$). Similarly, treatment with light alone (12 J/cm^2 and 24 J/cm^2) resulted to insignificant changes: 99.63% ± 0.203 and 95.93% ± 3.467, respectively. Treatment with 36 J/cm^2 of light alone resulted to produced 83.33% ± 2.333 of viable cells ($p < 0.05$). AE (2.5 μM, 5 μM, and 10 μM) with light (12 J/cm^2, 24 J/cm^2, and 36 J/cm^2) significantly reduced the cell viability in a PS and energy dose-dependent manner. AE (5 μM) and light (24 J/cm^2) which yielded 37.68 ± 0.81% of viable cells was chosen as the optimum condition for subsequent assays. No significant change was observed in the negative control cells, with or without DMSO treatment, at the various energy doses tested (Figure 2(b)).

3.2. Influence of AE-Mediated PDT on Apoptotic, Antiapoptotic, and Antitumor-Associated Proteins. As demonstrated in Figures 3(a) and 3(b), cleaved caspase 3 was significantly increased in the AE-mediated PDT group compared to the control group. AE or irradiation alone demonstrated insignificant cleaved caspase 3 elevation. Contrastingly, antiapoptotic protein Bcl-2 was significantly suppressed after AE-mediated PDT compared to the untreated group (as shown in Figure 3(c)). However, the suppression in the single treatment group for Bcl-2 was insignificant ($p > 0.05$). The p53 expression assessment revealed significant increase in AE-mediated PDT vis-a-vis the control group, demonstrating a significant change (as shown in Figure 3(d)). The single treatment groups also showed a lower increment ($p < 0.05$) than the AE-mediated PDT group.

3.3. AE-Mediated PDT Induces Apoptosis. Neither Annexin V nor 7-AAD stained cells were detectable in the untreated control group (P-L-) (Figure 4(a)). Besides, both Annexin V and 7-AAD positive cells were undetectable in the case of single treatment with either AE (P+L-) or PDT (P-L+). However, as shown in Figure 4(b), substantial cell proportion

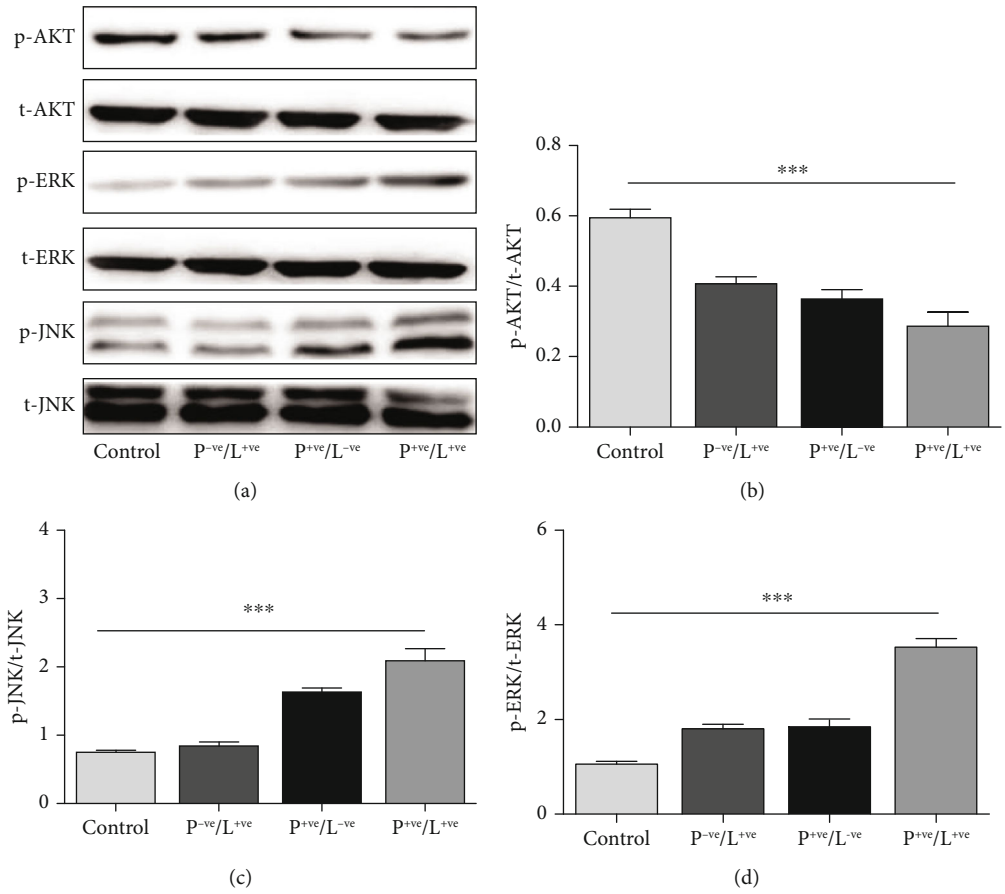

Figure 6: Effect of AE-mediated PDT on the Akt pathway and mitogen-activated protein kinases. (a) Western blotting analysis of Akt, JNK, and ERK following AE-PDT. The cells were treated with 5 μM AE, irradiated for 10 min, and protein lysates were collected 12 h later for western blotting assays. β-Actin was used as an internal control. The graphs represent the quantitative analysis of the change of (b) p-Akt, (c) p-JNK, and (d) p-ERK ($^{***}p < 0.0001$). Protein level was expressed as mean ± SD from three independent experiments.

was in the early apoptotic stage, as confirmed by Annexin V single positive cells. Further, a significant proportion of Annexin V and 7-AAD positive cell increase was observable in the AE-mediated PDT cells, as shown in Figure 4(c), explicitly confirming the occurrence of apoptosis.

3.4. AE-Mediated PDT Induces Intrinsic Apoptotic Pathway and Suppresses NF-κB. We aimed at investigating whether the killing initiated by AE-mediated PDT occurs intrinsically. Western blotting assay revealed significant cytochrome C increase in the AE-mediated PDT group compared to the negative control group (P-L-) (Figures 5(a) and 5(b)). On the other hand, phosphorylated NF-κB protein analysis showed a significant suppression following AE-PDT (Figure 5(c)). No change in total NF-κB was observed across the treatments.

3.5. Akt Pathway Signaling in AE-Mediated PDT Induced Cell Death. We aimed at elucidating the pathway involved during AE-mediated PDT cell death. Since the Akt pathway is important in cancer cell survival, we investigated expression levels of total Akt and its phosphorylated products. While the expression of total Akt was not changed across the various treatment groups, phosphorylated Akt was significantly reduced following AE-mediated PDT (Figures 6(a) and 6(b)).

3.6. Effect of AE-Mediated PDT on Mitogen-Activated Protein Kinases. We then investigated two MAPK families (extracellular signal-regulated kinases (ERKs) and C-Jun N-terminal kinases (JNKs)) to understand their involvement during PDT-mediated apoptosis. As shown in Figure 6(a), AE-mediated PDT significantly enhanced the phosphorylation of JNK ($p < 0.001$). No significant alteration of total JNK expression was noted in the single treatment groups (Figure 6(c)). Similarly, AE and PDT enhanced ERK phosphorylation with a significantly increased expression than the control group (Figure 6(d)). Expression of total ERK was not altered across the groups.

3.7. AE-Mediated PDT Induces Intracellular ROS Generation. We finally investigated the emission of fluorescence by H2DCFDA in a flow cytometer as means of ROS quantification. The outcome revealed a significant increase of ROS in AE-mediated PDT cells compared to the control and single treatment cells (Figures 7(a) and 7(b)).

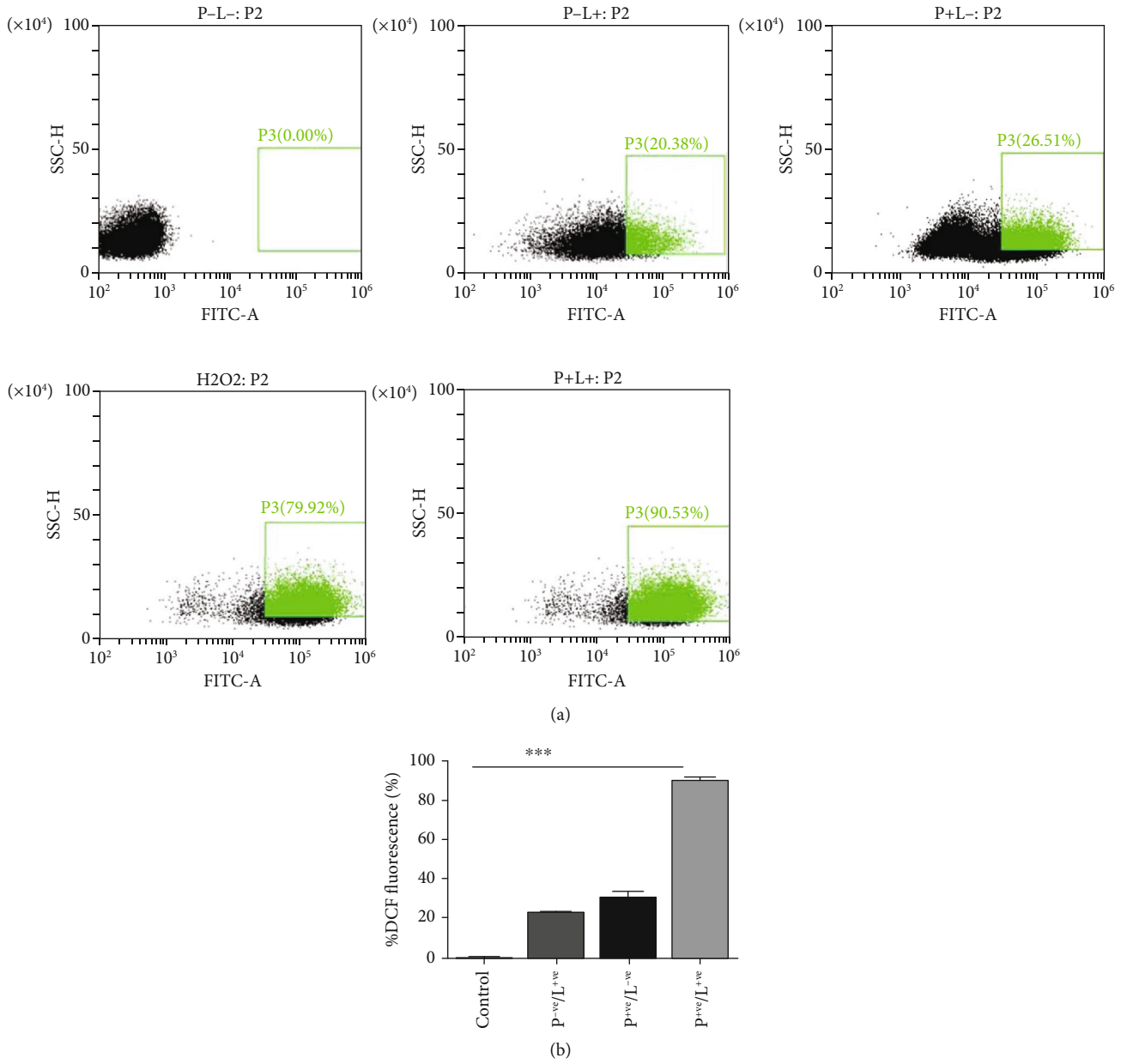

Figure 7: AE-mediated PDT induced intracellular ROS in TE 354.T cells. (a) Untreated cells (P-L-), light-treated cells (P-L+), AE-treated cells (P+L-), H_2O_2-treated positive control cells (H_2O_2), and AE-mediated PDT-treated cells (P+L-). (b) Bar graph representation of percentage fluorescence. Results are expressed as means ± SD from three independent assays.

4. Discussion

Conventionally, BCC has been treated through chemotherapy and surgery. However, these approaches are expensive, can lead to resistance and remissions, and may interfere with the skin cosmetic value. Surgery can also be challenging when the wounds are large or appear in the midface region [18]. PDT is a well tolerable, relatively painless, and inexpensive alternative [19]. Various PSs have been reported against BCC, for instance, mesotetrahydroxyphenylchlorin (mTHPC), hematoporphyrin derivative IX (Photoheme), 2-(1-hexyloxyethyl)-2-devinyl pyropheophorbide-a (HPPH), and benzoporphyrin derivative monoacid ring A (BPD-MA) [20, 21]. However, these PSs have the maximum absorption band in the red region; hence, their use with red light may result to fistula and perforations of walls [15]. As a PS with a shorter wavelength, AE could be suitable for the treatment of superficial BCC, without causing damage to the deeper healthy tissues.

This study confirmed the photocytotoxic effect of AE in combination with white light irradiation (435 ± 10 nm) against BCC, which occurs in an AE concentration and irradiation energy dose-dependent manner. AE at a concentration of 2.5 μM in the presence of 12 J/cm^2 and 24 J/cm^2 light all demonstrated an insignificant change of cell viabilities at 77.7 ± 0.847% and 62.517 ± 4.17%, respectively,

while 36 J/cm^2 of light significantly changed viability of cells to 39.88 ± 2.755%. AE at 5 μM easily inactivated BCC, with 24 J/cm^2, with cell viability yield of 37.697 ± 0.81%. Over 50% reduction in viability was observed when 10 μM AE was used with the various energy doses 12 J/cm^2, 24 J/cm^2, and 36 J/cm^2, which yielded 33.35 ± 1.219%, 26.48 ± 0.578 %, and 23.847 ± 1.07% cells, respectively. Consequently, this study notes that the ideal PDT condition for BCC inhibition is 5 μM and 24 J/cm^2.

According to our findings, AE-mediated PDT is more cytotoxic to TE 354.T cells than to MG63 or HUVEC cells [12]. Additionally, apoptosis was essentially the main mode of BCC cell death. We also found the results to be consistent with intracellular ROS changes, which were significantly and rapidly produced following AE-mediated PDT. These observations confirm that BCC cytotoxicity post-PDT is driven by the intracellular ROS production.

The p53 is a tumor suppressor, thus initiated apoptosis. Contrastingly, the observed Bcl-2 photodamage was due to mitochondrial destruction [22] and regulation by p53. Our finding is further supported by reports of downregulated Bcl-2 following MAL-PDT in cervical cancer cell lines [23].

Increased cytochrome C, cleaved caspase 3, and NF-κB expression shows that AE-mediated PDT initiates intrinsic apoptosis. As supported by previous research, cytochrome C is released into the cytosol from the mitochondria and triggers the cleaved caspase 3 [24]. Even though we did not study caspase 9 expression, it is an essential mitochondrial pathway determinant, whose increment is most likely in agreement with caspase 3 [25]. We consequently believed that cytochrome C and caspase 3 elevation firmly pointed to an intrinsic pathway initiated by AE-mediated PDT.

We further scrutinised NF-κB expression as a critical signal integrated by mitochondria in intrinsic apoptosis [26]. As a suppressor of apoptosis, NF-κB expression was significantly inhibited [27], thus downregulated by p53. Additionally, AE-mediated PDT causes redox modification upon exposure to severe oxidative stress [28], which could have also lead to reduced NF-κB.

Akt, as a serine/threonine kinase, enhances cells' survival through apoptosis inhibition and modulation of cellular growth factors [29]. Its phosphorylation occurs following activation by PI3K, and the consequence is proapoptotic Bcl-2 protein family function inhibition, hence cancerous cell survival. Our findings thus demonstrated a significantly downregulated p-Akt-level post-AE-mediated PDT. Its containment thus implied a successful apoptosis.

JNK and ERK are essential MAPK superfamily protein signaling due to their roles in growth regulation, apoptosis, survival, or differentiation [30]. ERK participates in transcription factor activation, for instance, c-myc (transcriptional regulator Myc-like), CREB (cAMP response element-binding proteins), and the NF-κB, an essential antitumor inhibitor [31–33]. However, according to our findings, AE-mediated PDT activated p-ERK, disputing the previous findings of 5-ALA, photofrin [34], and sulphoraphene-mediated PDT [35]. Nevertheless, our finding confirms previous reports of raised p-ERK following photofrin [36], TTPS2a [37], and 5-ALA-mediated PDT [38]. Worth noting, TTPS2a-PDT activated p-ERK in the presence of epidermal growth factor (EGF), which makes it digress from our design. At the same time, the other stated studies with similar findings do not give any clear explanation. To justify our finding of p-ERK activation upon AE-mediated PDT, we would agree with a postulation that ERK activation may depend on the cell type and the duration of phototherapy [39]. We thus report that AE-mediated PDT leads to activation of p-ERK on BCC.

Lastly, we report an increased p-JNK upon AE-mediated PDT, in agreement with previous investigations [24, 28, 40]. JNK is ascertained to be sparked by various environmental stresses such as irradiation, which activates various transcription factors as p53 and c-Jun, which most likely lead to cancerous cell death.

5. Conclusion

In conclusion, this study confirmed that AE in combination with 435 ± 10 nm light is cytotoxic against BCC in an AE concentration and light energy dose-dependent manner. Inactivation of BCC post-PDT is solely driven by the rapid production of intracellular ROS. Activation of both JNK and ERK1/2 and inhibition of the Akt pathway together played a role in enhancing the therapeutic response of AE-mediated PDT in the killing of basal skin cancer cells. These findings confirm that AE is a promising PS for the photodynamic inactivation of TE 354.T cells and may provide insight and guidance on a modal therapeutic approach of enhancing cytotoxicity against basal cell carcinoma in a clinical setting.

Abbreviations

BCC: Basal cell carcinoma
DMSO: Dimethyl sulfoxide
ERK: Extracellular signal-regulated kinase
PS: Photosensitizer
PDT: Photodynamic therapy
ROS: Reactive oxygen species
JNKs: Jun N-terminal kinases.

Data Availability

Most of the data generated in the study are included in this submission. The remaining raw data are available and can be provided by the corresponding author on request.

Conflicts of Interest

There is no conflict of interest to declare.

Acknowledgments

The authors acknowledge the National Natural Science Foundation of China (81401710 and 81670157) and the Natural Science Basic Research Plan in Shaanxi Province of China (Program No. 2020JM-052) as the providers of research funds.

References

[1] P. Agostinis, K. Berg, K. A. Cengel et al., "Photodynamic therapy of cancer: an update," *Cancer Journal of Clinicians*, vol. 61, no. 4, pp. 250–281, 2011.

[2] N. R. Telfer, G. B. Colver, C. A. Morton, and British Association of D, "Guidelines for the management of basal cell carcinoma," *The British Journal of Dermatology*, vol. 159, no. 1, pp. 35–48, 2008.

[3] E. Kasumagic-Halilovic, M. Hasic, and N. Ovcina-Kurtovic, "A clinical study of basal cell carcinoma," *Medical Archives*, vol. 73, no. 6, pp. 394–398, 2019.

[4] D. P. Kim, K. J. B. Kus, and E. Ruiz, "Basal cell carcinoma review," *Hematology/Oncology Clinics of North America*, vol. 33, no. 1, pp. 13–24, 2019.

[5] X. Wu, E. E. Elkin, and A. A. Marghoob, "Burden of basal cell carcinoma in USA," *Future Oncology*, vol. 11, no. 22, pp. 2967–2974, 2015.

[6] S. R. Lucena, A. Zamarrón, E. Carrasco et al., "Characterisation of resistance mechanisms developed by basal cell carcinoma cells in response to repeated cycles of photodynamic therapy," *Scientific Reports*, vol. 9, no. 1, article 4835, 2019.

[7] D. van Straten, V. Mashayekhi, H. S. de Bruijn, S. Oliveira, and D. J. Robinson, "Oncologic photodynamic therapy: basic principles, current clinical status and future directions," *Cancers (Basel)*, vol. 9, no. 12, p. 19, 2017.

[8] P. Savoia, T. Deboli, A. Previgliano, and P. Broganelli, "Usefulness of photodynamic therapy as a possible therapeutic alternative in the treatment of basal cell carcinoma," *International Journal of Molecular Sciences*, vol. 16, no. 10, pp. 23300–23317, 2015.

[9] H. E. Yoon, S. H. Oh, S. A. Kim, J. H. Yoon, and S. G. Ahn, "Pheophorbide a-mediated photodynamic therapy induces autophagy and apoptosis via the activation of MAPKs in human skin cancer cells," *Oncology Reports*, vol. 31, no. 1, pp. 137–144, 2014.

[10] C. Matei, M. Tampa, T. Poteca et al., "Photodynamic therapy in the treatment of basal cell carcinoma," *Journal of Medicine and Life*, vol. 6, no. 1, pp. 50–54, 2013.

[11] F. Vargas, Y. Díaz, and K. Carbonell, "Antioxidant and scavenging activity of emodin, aloe-emodin, and rhein on free-radical and reactive oxygen species," *Pharmaceutical Biology*, vol. 42, no. 4-5, pp. 342–348, 2004.

[12] Q. Chen, K. T. Li, S. Tian et al., "Photodynamic therapy mediated by aloe-emodin inhibited angiogenesis and cell metastasis through activating MAPK signaling pathway on HUVECs," *Technology in Cancer Research & Treatment*, vol. 17, 2018.

[13] Y. Q. Liu, P. S. Meng, H. C. Zhang et al., "Inhibitory effect of aloe emodin mediated photodynamic therapy on human oral mucosa carcinoma in vitro and in vivo," *Biomedicine & Pharmacotherapy = Biomedecine & Pharmacotherapie*, vol. 97, pp. 697–707, 2018.

[14] K. T. Li, Q. Chen, D. W. Wang et al., "Mitochondrial pathway and endoplasmic reticulum stress participate in the photosensitizing effectiveness of AE-PDT in MG63 cells," *Cancer Medicine*, vol. 5, no. 11, pp. 3186–3193, 2016.

[15] W. Ma, C. Liu, J. Li, M. Hao, Y. Ji, and X. Zeng, "The effects of aloe emodin-mediated antimicrobial photodynamic therapy on drug-sensitive and resistant Candida albicans," *Photochemical & Photobiological Sciences*, vol. 19, no. 4, pp. 485–494, 2020.

[16] L. Zang, H. Zhao, X. Ji, W. Cao, Z. Zhang, and P. Meng, "Photophysical properties, singlet oxygen generation efficiency and cytotoxic effects of aloe emodin as a blue light photosensitizer for photodynamic therapy in dermatological treatment," *Photochemical & Photobiological Sciences: Official journal of the European Photochemistry Association and the European Society for Photobiology*, vol. 16, no. 7, pp. 1088–1094, 2017.

[17] W. G. Wamer, P. Vath, and D. E. Falvey, "In Vitro studies on the photobiological properties of aloe emodin and aloin A," *Free Radical Biology and Medicine*, vol. 34, no. 2, pp. 233–242, 2003.

[18] W. Jerjes, Z. Hamdoon, and C. Hopper, "Photodynamic therapy in the management of basal cell carcinoma: retrospective evaluation of outcome," *Photodiagnosis and Photodynamic Therapy*, vol. 19, pp. 22–27, 2017.

[19] N. J. Collier, A. K. Haylett, T. H. Wong et al., "Conventional and combination topical photodynamic therapy for basal cell carcinoma: systematic review and meta-analysis," *The British Journal of Dermatology*, vol. 179, no. 6, pp. 1277–1296, 2018.

[20] S. Anand, B. J. Ortel, S. P. Pereira, T. Hasan, and E. V. Maytin, "Biomodulatory approaches to photodynamic therapy for solid tumors," *Cancer Letters*, vol. 326, no. 1, pp. 8–16, 2012.

[21] P. Baas, A. E. Saarnak, H. Oppelaar, H. Neering, and F. A. Stewart, "Photodynamic therapy with meta-tetrahydroxyphenylchlorin for basal cell carcinoma: a phase I/II study," *The British Journal of Dermatology*, vol. 145, no. 1, pp. 75–78, 2001.

[22] C. Lange, C. Lehmann, M. Mahler, and P. J. Bednarski, "Comparison of cellular death pathways after mTHPC-mediated photodynamic therapy (PDT) in five human cancer cell lines," *Cancers (Basel)*, vol. 11, no. 5, p. 702, 2019.

[23] G. F. He, M. L. Bian, Y. W. Zhao, Q. Xiang, H. Y. Li, and C. Xiao, "A study on the mechanism of 5-aminolevulinic acid photodynamic therapy in vitro and in vivo in cervical cancer," *Oncology Reports*, vol. 21, no. 4, pp. 861–868, 2009.

[24] P. Mroz, A. Yaroslavsky, G. B. Kharkwal, and M. R. Hamblin, "Cell death pathways in photodynamic therapy of cancer," *Cancers (Basel)*, vol. 3, no. 2, pp. 2516–2539, 2011.

[25] H. D. Lin, K. T. Li, Q. Q. Duan et al., "The effect of aloe-emodin-induced photodynamic activity on the apoptosis of human gastric cancer cells: a pilot study," *Oncology Letters*, vol. 13, no. 5, pp. 3431–3436, 2017.

[26] B. C. Albensi, "What is nuclear factor kappa B (NF-κB) doing in and to the mitochondrion?," *Frontiers in Cell and Development Biology*, vol. 7, p. 154, 2019.

[27] L. Bernal-Mizrachi, C. M. Lovly, and L. Ratner, "The role of NF-{kappa}B-1 and NF-{kappa}B-2-mediated resistance to apoptosis in lymphomas," *Proceedings of the National Academy of Sciences of the United States of America*, vol. 103, no. 24, pp. 9220–9225, 2006.

[28] M. Broekgaarden, R. Weijer, T. M. van Gulik, M. R. Hamblin, and M. Heger, "Tumor cell survival pathways activated by photodynamic therapy: a molecular basis for pharmacological inhibition strategies," *Cancer Metastasis Reviews*, vol. 34, no. 4, pp. 643–690, 2015.

[29] G. M. Nitulescu, M. van de Venter, G. Nitulescu et al., "The Akt pathway in oncology therapy and beyond (review)," *International Journal of Oncology*, vol. 53, no. 6, pp. 2319–2331, 2018.

[30] C. Braicu, M. Buse, C. Busuioc et al., "A comprehensive review on MAPK: a promising therapeutic target in cancer," *Cancers (Basel)*, vol. 11, no. 10, p. 1618, 2019.

[31] J. McCain, "The MAPK (ERK) pathway: investigational combinations for the treatment of BRAF-mutated metastatic melanoma," *Pharmacy and Therapeutics*, vol. 38, no. 2, pp. 96–108, 2013.

[32] J. Piette, "Signalling pathway activation by photodynamic therapy: NF-κB at the crossroad between oncology and immunology," *Photochemical & Photobiological Sciences: Official Journal of the European Photochemistry Association and the European Society for Photobiology*, vol. 14, no. 8, pp. 1510–1517, 2015.

[33] J. Guo, B. Xiao, Q. Liu, Z. Gong, and Y. Le, "Suppression of C-myc expression associates with anti-proliferation of aloe-emodin on gastric cancer cells," *Cancer Investigation*, vol. 26, no. 4, pp. 369–374, 2008.

[34] T. W. Wong, E. Tracy, A. R. Oseroff, and H. Baumann, "Photodynamic therapy mediates immediate loss of cellular responsiveness to cytokines and growth factors," *Cancer Research*, vol. 63, no. 13, pp. 3812–3818, 2003.

[35] S. Chatterjee, Y. Rhee, P. S. Chung, R. F. Ge, and J. C. Ahn, "Sulforaphene enhances the efficacy of photodynamic therapy in anaplastic thyroid cancer through Ras/RAF/MEK/ERK pathway suppression," *Journal of Photochemistry and Photobiology. B*, vol. 179, pp. 46–53, 2018.

[36] Z. Tong, G. Singh, and A. J. Rainbow, "Sustained activation of the extracellular signal-regulated kinase pathway protects cells from photofrin-mediated photodynamic therapy," *Cancer Research*, vol. 62, no. 19, pp. 5528–5535, 2002.

[37] A. Weyergang, O. Kaalhus, and K. Berg, "Photodynamic therapy with an endocytically located photosensitizer cause a rapid activation of the mitogen-activated protein kinases extracellular signal-regulated kinase, p38, and c-Jun NH2 terminal kinase with opposing effects on cell survival," *Molecular Cancer Therapeutics*, vol. 7, no. 6, pp. 1740–1750, 2008.

[38] X. Ge, J. Liu, Z. Shi et al., "Inhibition of MAPK signaling pathways enhances cell death induced by 5-aminolevulinic acid-photodynamic therapy in skin squamous carcinoma cells," *European Journal of Dermatology*, vol. 26, no. 2, pp. 164–172, 2016.

[39] R. Thamkachy, R. Kumar, K. N. Rajasekharan, and S. Sengupta, "ERK mediated upregulation of death receptor 5 overcomes the lack of p53 functionality in the diaminothiazole DAT1 induced apoptosis in colon cancer models: efficiency of DAT1 in Ras-Raf mutated cells," *Molecular Cancer*, vol. 15, no. 1, p. 22, 2016.

[40] Y. Xu, D. Wang, Z. Zhuang et al., "Hypericin-mediated photodynamic therapy induces apoptosis in K562 human leukemia cells through JNK pathway modulation," *Molecular Medicine Reports*, vol. 12, no. 5, pp. 6475–6482, 2015.